A Screening Approach for Identifying Co-crystal Types and Resolution Opportunities in Complex Chiral Multicomponent Systems

Weiwei Li[1], Mariette de Groen[1], Herman J.M. Kramer[1], René de Gelder[2], Paul Tinnemans[2], Hugo Meekes[2] and Joop H. ter Horst[3]*

[1] Delft University of Technology, Department of Process and Energy, Leeghwaterstraat 39, 2628 CB, Delft, The Netherlands

[2] Radboud University, Institute for Molecules and Materials, Heyendaalseweg 135, 6525 AJ Nijmegen, The Netherlands

[3] University of Strathclyde, EPSRC Centre for Innovative Manufacturing in Continuous Manufacturing and Crystallisation (CMAC), Strathclyde Institute of Pharmacy and Biomedical Sciences, Technology and Innovation Centre, 99 George Street, Glasgow G1 1RD, United Kingdom.

Abstract: Co-crystallization of racemic-compound-forming chiral molecules can result in conglomerate co-crystals or diastereomerically related co-crystals, which enable the application of chiral separation techniques such as preferential crystallization and classic resolution. Here, a systematic method to identify the types and phase diagrams of co-crystals formed by chiral target compounds and candidate co-formers in a particular solvent system is presented, which allows the design of suitable chiral resolution processes. The method is based on saturation temperature measurements of specific solution compositions containing both enantiomers of chiral molecules and a co-former. This method is applied to analyze three different systems. For racemic Phenylalanine (Phe) in water/ethanol mixtures one of the enantiomers selectively co-crystallizes with the opposite enantiomer of Valine (Val), forming the more stable diastereomerically related co-crystal. The racemic compound Ibuprofen crystallizes with the non-chiral co-former 1,2-Bis(4-pyridyl)ethane (BPN) as racemic compound co-crystals. More interestingly, when combined with trans-1-(2-pyridyl)-2-(4-pyridyl)-ethylene (BPE), the racemic compound Ibuprofen co-crystallizes as a conglomerate, which in principle enables the application of preferential crystallization of this racemic compound. The systematic method shows the benefit of using pseudo-binary phase diagrams. Such pseudo-binary phase diagrams depict the saturation temperature on a very specific route through the quaternary phase diagram, allowing the identification of various co-crystal types as well as the corresponding co-crystallization conditions. The systematic method can be used to identify a suitable solid phase for chiral separation and the obtained phase diagram information enables to perform a crystallization-mediated chiral resolution process design.

Such a guideline for a chiral resolution process design has never been reported for conglomerate co-crystal systems such as IBU:BPE, presented in this study.

*Joop H. ter Horst; E-mail: Joop.terHorst@strath.ac.uk.

99 George Street, Glasgow G1 1RD, United Kingdom

1. INTRODUCTION

Enantiomers of chiral products possess both pharmacological and toxicological differences. The awareness of such differences has driven the development towards new chiral separation techniques.[1-2] Chiral separation techniques such as preferential crystallization and Viedma ripening are now effective and efficient in achieving high enantiopurity for specific scientific examples of chiral products.[1, 3-5] The general industrial application of these techniques requires the target compounds to form crystals which only contain a single enantiomer. However, in the substantial majority of the cases the two enantiomers of a chiral compound together form a solid (racemic compound) which significantly limits the application of chiral separation techniques.[6]

To overcome this drawback, various approaches can be followed to enable chiral separation through a solid state conversion. A racemic compound-forming chiral compound can be chemically modified into derivatives that crystallize as conglomerates. For instance, Naproxen has been successfully deracemized via its conglomerate ester derivatives.[7] Salt and solvate formation, for instance the ethanolamine salt of Mandelic acid and the monohydrate of Asparagine, can also provide the opportunity to convert a racemic compound to a conglomerate.[8-10] Alternatively, co-crystallization can modify the solid phase of target compounds for the application of separation techniques[11-13], for instance by converting racemic compounds into conglomerate co-crystals for chiral separation[14-15]. Up till now, the conglomerate co-crystal system of Naproxen—Nicotinamide and Ibuprofen— trans-1-(2-pyridyl)-2-(4-pyridyl)-ethylene (BPE) are the only two reported in literature.[16-17] Additionally, conglomerate co-crystal hydrates, for instance the salicylic acid monohydrate of proxyphylline, have been reported[18]. Such co-crystal hydrate systems can also enable the chiral separation of racemic compounds[19], but they will not be further discussed here, as the present study focuses on the binary system of chiral molecules and their co-formers.

Various co-crystal types can be formed when combining a racemic compound and a co-former into co-crystals. Co-crystals are crystals containing two or more neutral non-solvent molecular components in the same crystal lattice.[20] Successful chiral co-formers form two distinct diastereomerically related co-crystals with the enantiomers (see co-crystal type 1 in Scheme 1). The two enantiomers could be separated based on solubility differences between diastereomeric co-crystals or between the co-crystals and the pure component crystals.[21-22] On the other hand, an achiral co-former can co-crystallize with a racemic compound into either conglomerate or racemic compound co-crystals (see co-crystal type 2 and 3 in Scheme 1, respectively), and the former type paves the way to the application of chiral separation techniques such as preferential crystallization on racemic compound via co-crystallization.[16, 23] In much rarer cases, solid solution co-crystals are formed between an achiral co-former and a racemic compound, which contain random amounts of the two enantiomers in the lattice[24]. In the present study, solid solution co-crystals are not discussed due to their rarity. A systematic screening method to identify the various co-crystal types in these complex multicomponent chiral systems benefits the selection and design of a suitable chiral separation process.

The phase diagram of a multi-component system provides information about the compositions in the various phases. However, a complete phase diagram for a quaternary system containing both enantiomers, a co-former and a solvent, which also includes temperature as a variable, exists only in four-dimensional space. The construction of such a quaternary phase diagram requires large numbers of measurements, slowing down the efficient screening of suitable co-formers for the target compound.[25] A projection of the interesting part of such a phase diagram on a two-dimensional plane, a pseudo-binary phase diagram, can identify co-crystal formation as well as the co-crystal type with significantly less measurements, thus suitable as a screening tool.

In this study, a systematic method using pseudo-binary phase diagrams is presented for identifying the co-crystal types formed using a racemic compound and a candidate co-former. The method is experimentally verified as a useful screening procedure prior to the design and operation of a co-crystallization-mediated chiral separation process.

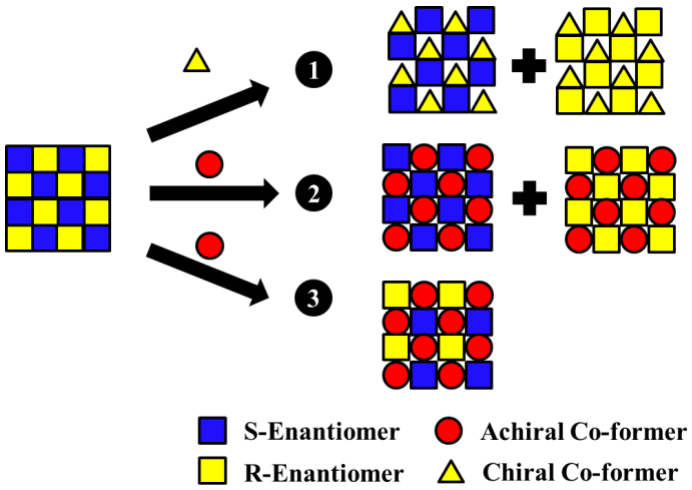

Scheme 1. Schematic demonstration of co-crystal types using a racemic compound (blue and yellow squares) and a chiral (yellow triangle) or achiral (red circle) co-former: (1) diastereomerically related co-crystals; (2) conglomerate co-crystals and (3) racemic compound co-crystals. For convenience we ignored formation of relatively rare solid solutions.

2. EXPERIMENTAL

Materials. Racemic Ibuprofen (RS-IBU, 99%) and trans-1-(2-pyridyl)-2-(4-pyridyl)-ethylene (BPE, 98%) were obtained from Santa Cruz Biotechnology. S-Ibuprofen (S-IBU, 99%), 1,2-Bis(4-pyridyl)ethane (BPN, 99%), Heptane (99%), S-Phenylalanine (S-Phe, ≥ 99.0%), R-Phenylalanine (R-Phe, ≥ 98.0%), RS-Phenylalanine (RS-Phe, ≥ 99.0%), R-Valine (R-Val, ≥ 98.0%), S-Valine (S-Val, ≥ 98.0%), RS-Valine (DL-Val, ≥ 99.0%) and ethanol were

supplied by Sigma Aldrich. All chemicals were used without further purification. Molecular structures of Val, Phe, IBU, BPN and BPE are shown in Figure 1.

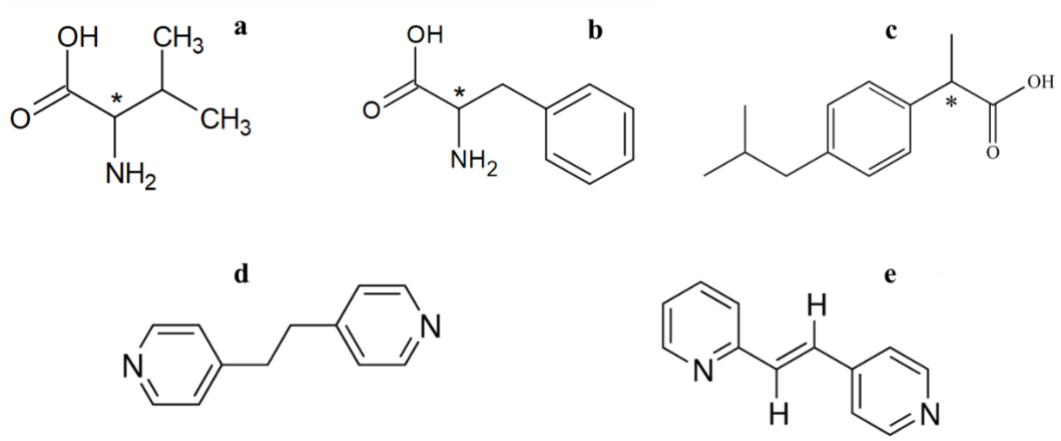

Figure 1. Molecular structures of Val (a), Phe (b), IBU (c), BPN (d) and BPE (e). Asterisks in a—c show the locations of the chiral centers.

From this point onwards we will adopt the RS notation for the amino acids, meaning that D-Phe corresponds to R-Phe and D-Val corresponds to R-Val. This is done for consistency in notation throughout the paper.

Solubility Measurement. Crystal16 equipment (Technobis B.V.) was used for all saturation temperature measurement in this study, following a method developed by ter Horst et al[26]. A suspension of a known composition x was prepared from the pure components and the corresponding solvent. The suspension was linearly heated (0.3°C/min) until full dissolution (clear point) and then linearly cooled down (-0.3°C/min) for recrystallization. The clear point temperature was noted as the saturation temperature T_s of the corresponding composition. The heating-cooling cycle was repeated for three times and the average T_s was taken to represent the saturation temperature of the sample composition.

Saturation temperature of mixed compositions. A series of mixed samples were prepared containing the target compound (either its racemic form or the enantiopure form) and the co-former in order to determine co-crystal existence. The compositions of the target compound

(A) and the co-former (B) in the mixed samples were their equilibrium molar fractions $x_A^*(T_r)$ and $x_B^*(T_r)$ in the corresponding pure component solutions at various reference temperatures T_r, estimated from van 't Hoff equation (Equation 2). The measured $T_s(x_A^*(T_r), x_B^*(T_r))$ of the mixed samples were compared with T_r. Positive temperature differences $\Delta T = T_s - T_r$ indicate the appearance of a solid different from either pure compound A or B. Due to the possibility of non-ideal solutions we assigned an arbitrarily chosen $\Delta T > 10°C$ to indicate the existence of a stable co-crystal consisting of compound A and B.[26]

Type-I Phase Diagram. In a Type-I phase diagram, the sample composition (x_A, x_B) of the target compound A (either its racemic form or enantiopure form) and the co-former B is described by the following equation:

$$\frac{x_B}{x_B^*(T_r)} = 1 - \frac{x_A}{x_A^*(T_r)} \qquad \text{Equation 1}$$

where x_A and x_B are the molar fractions of the target compound (A) and the co-former (B), while x_A^* and x_B^* are the equilibrium molar fractions of A and B at a chosen temperature T_r in their corresponding pure component solution. The saturation temperatures T_s of such a series of samples was measured and plotted against the solvent-excluded molar fraction $y_B = x_B/(x_A + x_B)$, as a type I pseudo-binary phase diagram.

Type-II Phase Diagram. In order to identify racemic compound or conglomerate behavior of the co-crystals a Type-II phase diagram was determined. In the samples of a Type-II phase diagram, the total molar fraction of both enantiomers $x_A = x_R + x_S$ is chosen constant, as well as the molar fractions x_B and $1-x_A-x_B$ of co-former and solvent, respectively. This leaves the enantiomer fraction $y_S = x_S/(x_S + x_R)$ as a variable in the sample compositions. The measured saturation temperatures T_s for these samples with varying y_S but constant x_B and x were plotted against the molar fraction y_S of S-enantiomer in both enantiomers of the corresponding

samples. The sample compositions used in all type II phase diagrams in the present study are shown in Table. 1.

Two different solvent systems were used in the construction of type-II pseudo-binary phase diagrams. The selection of Ethanol/H_2O, in the case of amino acid phase diagrams, was to avoid fouling and scaling, which usually took place when pure Ethanol or water was used. Fouling and scaling negatively affect the accuracy of the solubility measurements. Heptane was used for the two systems from IBU, as it provided a not too high solubility for both racemic and enantiopure IBU, saving material and increasing the accuracy of the solubility measurements.

The composition ratio of the target amino acid and its co-former was decided by their corresponding single component solubility. Those between IBU and other two co-formers were selected based on trial-and-error, as the solubility of the co-formers could not be precisely measured, partially because the co-former crystals were floating on top of the liquid surface, which caused significant fluctuation in the laser signal of Crystal16.

It should be noted that the solid phase is dissolved in the tests of constructing the phase diagrams. Therefore, the nature of the solid of which the solubility is determined is not known with explicitly certainty. However, separate suspension tests allowed for confirmation of the presence of a co-crystal phase rather than the pure component crystal phases under conditions deduced from the phase diagrams.

Table 1. Molar compositions of samples for each Type-II pseudo-binary phase diagram. A = Target Compound, B = Co-former, Val = Valine, Phe = Phenyalanine, IBU = Ibuprofen, BPE = trans-1-(2-pyridyl)-2-(4-pyridyl)-ethylene and BPN = 1,2-Bis(4-pyridyl)ethane. Ethanol/H_2O solvent composition: 20/80 %v/v.

Experiment Nr.	Target Compound (A)	Co-former (B)	Solvent	x_A [mmol/mol]	x_B [mmol/mol]
1	RS-Val	-	Ethanol/H_2O	7.6	0
2	RS-Phe	-	Ethanol/H_2O	2.3	0
3	RS-Val	S-Phe	Ethanol/H_2O	7.6	2.3
4	RS-Phe	S-Val	Ethanol/H_2O	2.3	4.4
5	RS-IBU	-	Heptane	114	0
6	RS-IBU	BPE	Heptane	114	28
7	RS-IBU	BPN	Heptane	114	28

X-ray powder diffraction (XRPD) to identify the crystalline phase composition. After recrystallization, samples were filtered at room temperature and the obtained solid was analyzed by XRPD, carried out in a Bruker D2 Phaser (Bruker AXS GmbH, Karlsruhe, Germany). Data collection was done using monochromatic CuKα_1 radiation (λ = 0.154056 nm) in the 2θ region between 8° and 50°, with a 2θ step size of 0.022°. Data evaluation was done with the Bruker program EVA.

Construction of theoretical solubility lines in the Type-I and Type-II pseudo-binary phase diagrams. In order to estimate the solubility in the various phase diagrams used, a modified Van 't Hoff equation was used to account for solubility products:

$$\sum_{i}^{N} \ln x_i = -\frac{\Delta H}{R}\left(\frac{1}{T_s} - \frac{1}{T_0}\right) \qquad \text{Equation 2}$$

where x_i are the molar fraction of the component(s) i, forming the solid phase, N is the total number of components i, including enantiomers, in the co-crystals, T_s [K] is the saturation temperature and ΔH and T_0 [K] are parameters specific for each solubility line and phase diagram, estimated from corresponding experimental data. As an example, the Van 't Hoff parameters of the S-IBU-BPE co-crystal were estimated from the experimental T_s and the corresponding molar fraction product $x_{S\text{-}IBU} \cdot x_{BPE}$ (N=2 here as R-IBU is not in the enantiopure co-crystal). In the case of the co-crystal of RS-IBU–BPN, on the other hand, the molar fractions of both R- and S-IBU and of BPN were taken into account. Therefore, ΔH and T_0 of RS-IBU-BPN were estimated from experimental T_s and $x_{R\text{-}IBU} \cdot x_{S\text{-}IBU} \cdot x_{BPE}$ (N=3 here as both enantiomers and the co-former are in the co-crystals). The parameters of the Van 't Hoff equation were used to interpolate or extrapolate solubility of the target component at other temperatures, as well as to construct theoretical phase diagrams. It should be noted that the stoichiometry in the co-crystals is not taken into account in Equation 2, as the phase diagrams are to be constructed prior to the structural determination of the co-crystals of interest (see the procedure detail in Discussion).

Single-crystal X-ray diffraction (XRD) of co-crystals. Crystals of IBU-BPE suitable for X-ray diffraction were prepared by slowly evaporating an ethanol solution containing 510.3 mg/ml RS-IBU and 232.0 mg/ml BPE at 40°C. For single-crystal X-ray diffraction a crystal was coated with high viscosity oil, mounted on a Mitagen Microloop and shock frozen to 208K using liquid nitrogen. Intensity data were collected at 208K. The measurement was performed on a Nonius KappaCCD, φ and ω scans, using monochromated MoKα radiation.

Crystals of S-IBU-BPN suitable for X-ray diffraction were prepared by slowly evaporating an ethanol solution containing 19.9 mg/ml S-IBU and 17.9 mg/ml BPN at room temperature. For single-crystal X ray diffraction, a crystal was coated with high viscosity oil, mounted on a Mitagen Microloop and shock frozen to 150K using liquid nitrogen. Intensity data were

collected at 150K. The measurement was performed on a Bruker D8 Quest, φ scans, using monochromated MoKα radiation.

The structures were solved using CRUNCH[27] (IBU-BPE) and SHELXT[28] (S-IBU-BPN) and were refined with standard methods using SHELXL.[29] All non-hydrogen atoms were refined with anisotropic temperature factors. The positions of the hydrogen atoms could initially be determined using a difference Fourier map. Hydrogens were subsequently, when possible, replaced by hydrogens at calculated positions and refined riding on the parent atoms. The S-IBU-BPN co-crystal structure with formula $C_{38}H_{48}N_2O_4$ refined to $R1$ = 0.0403 for 6486 reflections with $Io > 2.0\ \sigma(Io)$. The IBU-BPE co-crystal structure with formula $C_{25}H_{28}N_2O_2$ refined to $R1$ = 0.0397 for 5602 reflections with $Io > 2.0\ \sigma(Io)$.

Table 2. Values of the van 't Hoff parameters in Equation 2 for each crystalline materials introduced in this study. Val = Valine, Phe = Phenyalanine, IBU = Ibuprofen, BPE = trans-1-(2-pyridyl)-2-(4-pyridyl)-ethylene and BPN = 1,2-Bis(4-pyridyl)ethane. The errors of the two parameters are standard deviations from fitting experimental data in the van 't Hoff equation.

Crystal Composition	Exp. Nr.	ΔH [kJ/mol]	T_0 [K]
S-Val	1	21.5 ± 1.7	792 ± 177
S-Phe	2	19.7 ± 0.8	1314 ± 237
RS-Val	1	29.2 ± 1.1	363 ± 104
RS-Phe	2	46.8 ± 0.9	927 ± 85
R-Val-S-Phe or S-Val-R-Phe	3 and 4	43.4 ± 0.8	1209 ± 86
RS-IBU	5	134.7 ± 4.0	351 ± 18
S-IBU	5	58.4 ± 0.5	311 ± 4
S-IBU-BPE	6	55.3 ± 1.6	487 ± 28
RS-IBU-BPN	7	57.7 ± 3.4	576 ± 78
S-IBU-BPN	7	22.1 ± 2.4	1102 ± 430

3. RESULTS

3.1. Diastereomerically Related Co-crystals using Chiral Co-formers

Phenylalanine (Phe) and Valine (Val) are amino acids with a single chiral center. Both amino acids are reported to crystallize as racemic compounds from racemic solutions. Interestingly, it has also been reported that S-Phe and R-Val can form a 1:1 co-crystal[30] while there are to our knowledge no reports on the diastereomerically related co-crystal with the same handedness of Phe and Val. Therefore, we chose to investigate the effect of the S-Val co-former for the RS-Phe system and the S-Phe co-former for the RS-Val system.

Pure Component Solubilities. Firstly, the solubilities of the pure components S-Val, RS-Val, S-Phe and RS-Phe in an 20/80 % v/v ethanol/water mixture were measured. The solubility is plotted as a function of temperature in Figure 2 (left) along with the corresponding Van 't Hoff plots in Figure 2 (right). While the data points of the other compounds gave a good fit to Equation 2, the solubility curve of S-Val showed a discontinuity near 42 mg/ml, which is possibly the result of S-Val polymorphism[31]. Since pure component polymorphism is not the focus of the study we did not further look into this. RS-Val shows a higher solubility than the enantiopure S-Val. At 50°C, the solubility of S-Val is 44.5 mg/ml, which is more than half of the solubility of RS-Val at the same temperature (58.7 mg/ml), indicating that RS-Val is a racemic compound. RS-Phe shows a much lower solubility than S-Phe, which indicates that RS-Phe is a highly stable racemic compound. At 40°C, the solubility of S-Phe is 25.7 mg/ml ($x_{\text{S-Phe}}$*(40°C) = 3.3 mmol/mol) and the solubility of RS-Phe is 13.3 mg/ml ($x_{\text{RS-Phe}}$*(40°C) = 1.7 mmol/mol). The experimental pure component solubilities were fitted to Equation 2 in

order to determine the Van 't Hoff parameters, which were used to estimate the phase diagrams of the model systems.

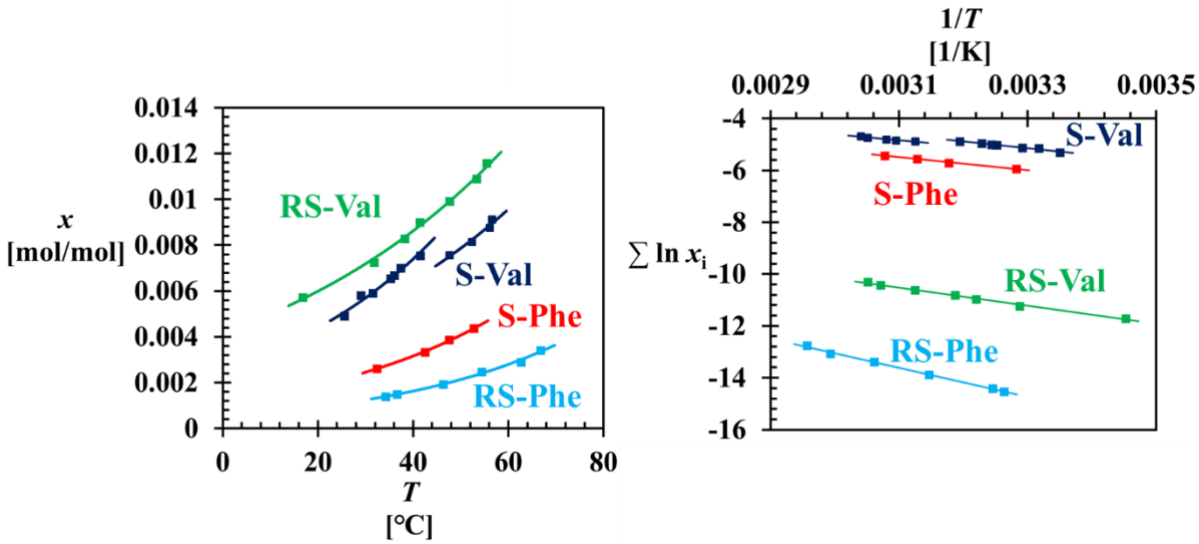

Figure 2. Left: Solubility of RS-Val, S-Val, RS-Phe and S-Phe in 20/80 % v/v ethanol/water (left) as a function of temperature. Right: The experimental data fitted to equation 2. The solid lines in both figures are theoretical solubilities estimated from Equation 2.

Saturation Temperatures of Co-crystal Systems. During a solution co-crystal screening, the composition with the highest possibility of forming a new co-crystalline material is not determined by the expected co-crystal stoichiometry but by the pure component solubilities[26]. Specifically, a system containing the target compound A and the co-former B of the composition [$x_A^*(T_r)$, $x_B^*(T_r)$] has the highest possibility of forming co-crystals A-B, where x_A^* and x_B^* are the equilibrium molar fractions of respectively A and B at a reference temperature T_r[26]. If a more stable co-crystal forms, the measured saturation temperature $T_s > T_r$ of such a composition is usually substantially higher than the reference temperature T_r, since the saturation temperature T_s is that of the more stable co-crystal rather than the pure component crystals[26].

Therefore, by measuring the temperature difference T_s - T_r new co-crystal materials constructed of the target molecule and the co-former can be identified[26]. Here the saturation

temperatures of a series of mixtures of S-Phe, as the chiral co-former, and either S- or R-Val, as the target molecule, were measured. In Figure 3, the determined temperature difference T_s - T_r is plotted against the chosen reference temperature T_r. The saturation temperatures T_s of the R-Val:S-Phe system are substantially higher than the corresponding reference temperatures T_r, strongly indicating the existence of R-Val:S-Phe co-crystals. On the contrary, the saturation temperatures of the S-Val:S-Phe were slightly lower than the corresponding reference temperatures, suggesting that no co-crystallization took place between the two compounds.

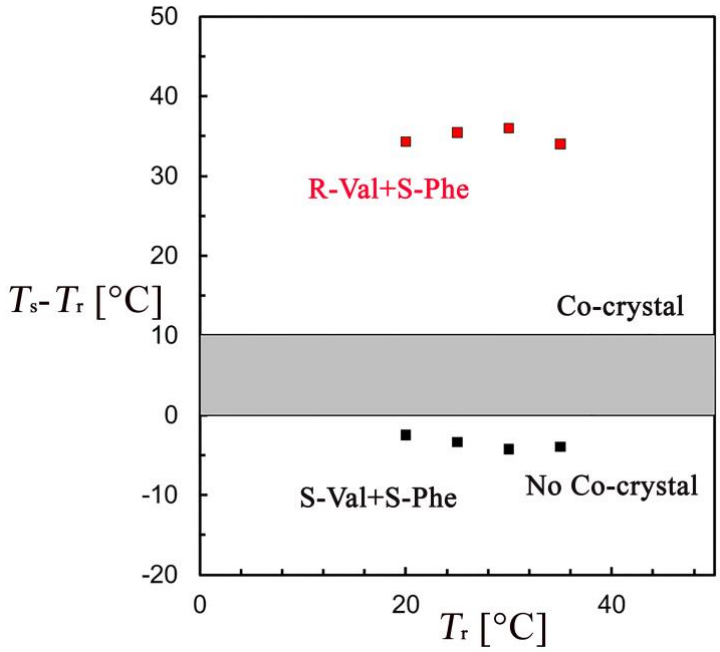

Figure 3. Difference T_s-T_r between saturation temperature T_s and reference temperature T_r of R-Val + S-Phe (red) and S-Val + S-Phe compositions (black) in 20/80 %v/v Ethanol/Water. The large positive difference (the region, where T_s-T_r > 10°C, above the grey area) indicates the existence of a stable co-crystalline phase for R-Val:S-Phe, while there is no indication for a stable co-crystal from S-Val and S-Phe.

Type-I Pseudo-binary Phase Diagrams. Chiral co-formers interact differently with the opposite enantiomers of the same chiral compound. The results in Figure 3 suggest that Phe only co-crystallizes with Val of the opposite chirality and vice versa. For further verification,

we investigated saturation temperature behavior for three component mixtures of S-Val, with either S- or R-Phe in 20/80 % v/v ethanol/water.

In the top of Figure 4 the specific compositions are schematically indicated in a compositional pyramid of the quaternary system of the 2 enantiomers, co-former B and solvent H. The red and green side-triangles of the pyramid describe compositions of mixtures containing H, B and one of the enantiomers of A following Equation 1. On the target compound side the lines start at the pure component solubilities $x_R^*(T_r)$ and $x_S^*(T_r)$ at reference temperature T_r. Both lines end at the pure component solubility $x_B^*(T_r)$ of the co-former B.

The lower left of Figure 4 shows the Type I pseudo-binary phase diagram of target compound S-Val and chiral co-former R-Phe in 20/80 % v/v ethanol/water. The Type I phase diagram is divided into three parts by two eutectic points. The two outer parts with decreasing saturation temperatures towards the middle indicate the saturation temperatures of solids of R-Phe and S-Val, the predicted saturation temperatures using the pure component solubility results are represented by the red and the black solid lines, respectively. The middle part ($0.3 < y_{Val} < 0.9$), which is significantly deviating from the theoretical saturation temperatures of the pure components, shows the composition region of a more stable co-crystal S-Val:R-Phe having higher saturation temperatures within that region.

The powder pattern of the collected crystals is distinctly different from those of both S-Val and R-Phe crystals. On the other hand, the powder patterns of the collected crystals and the reported[32] R-Val:S-Phe co-crystals are quite similar despite strong preferential orientation in our powder sample (see details in ESI). Therefore, the formed solid phase of the samples in this middle region is indeed the co-crystal S-Val:R-Phe.

The Type I pseudo-binary phase diagram of target compound S-Val and co-former S-Phe in the bottom right of Figure 4 shows that for the S-Val+S-Phe system no co-crystal region exists. The left part of the phase diagram indicates the solubility of S-Phe, of which the predicted

saturation temperatures are represented by a red line. When $y_{Val} > 0.7$, where S-Val is theoretically the more stable solid phase, no saturation temperatures could be measured since none of the samples recrystallized. It seems that S-Phe substantially inhibits the crystallization of S-Val.

The comparison between the two Type I phase diagrams in Figure 4, along with the results of the XRPD analysis, show that Phe and Val can only form stable co-crystals with each other if they possess opposite chiralities.

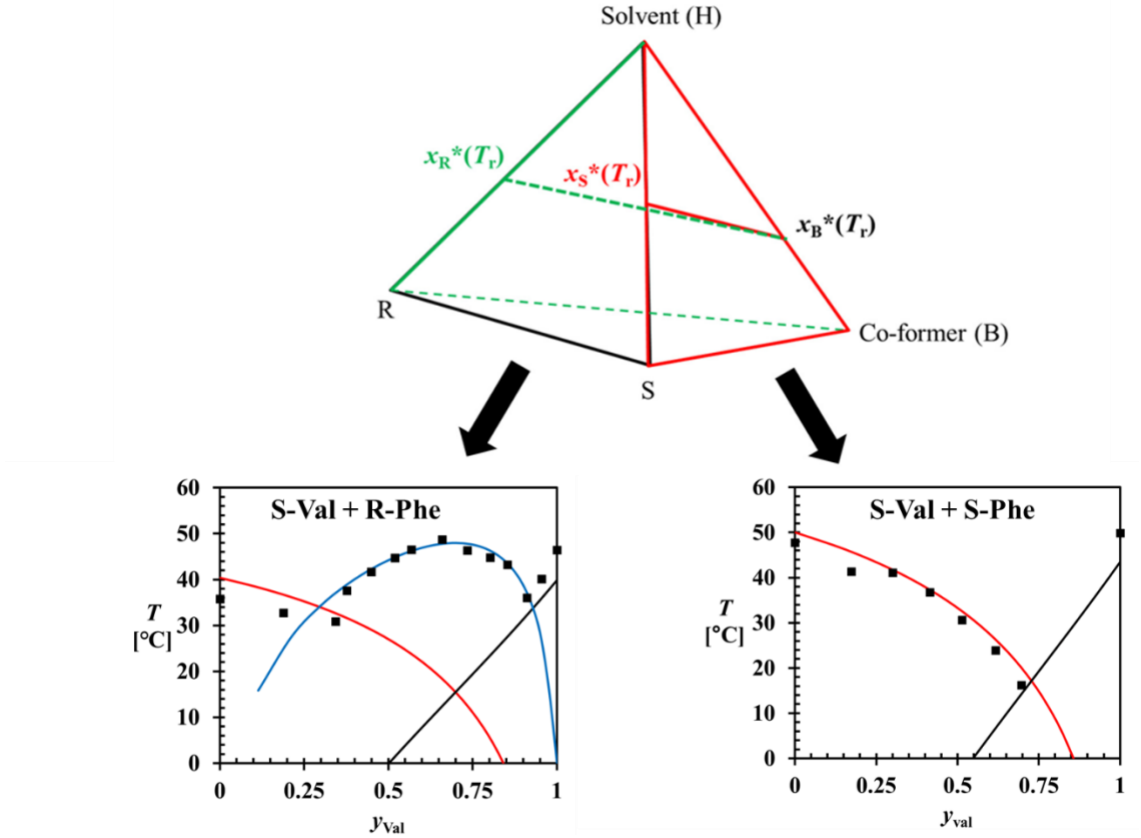

Figure 4. Top: Schematic demonstration of the compositional pyramid of a quaternary system of the target chiral compound consisting of enantiomers R and S, the co-former B and the solvent H. The lines (either solid or dashed) crossing the red and green pyramid side planes represent the compositions of the type-I pseudo-binary phase diagrams from H, B and one enantiomer of the target compound. Bottom: Type I pseudo-binary phase diagrams for the target enantiomer S-Val with co-former R-Phe at a reference temperature of 40°C (left) and for the target enantiomer S-Val with co-former S-Phe at a reference temperature of 50°C (right),

both in a 20/80 %v/v ethanol/water mixture showing the measured saturation temperatures T_s as a function of solvent-excluded molar fraction $y_{Val} = x_{Val}/(x_{Val}+x_{Phe})$. The molar compositions x_{Val} and x_{Phe} (for either S- or R-Phe) followed Equation. 1. Solid lines are predicted saturation temperatures of pure S-Val (black) and either S- or R-Phe (red) solutions from Equation. 2. The blue solid line is the theoretical saturation temperature of co-crystal S-Val:R-Phe estimated from Equation. 2.

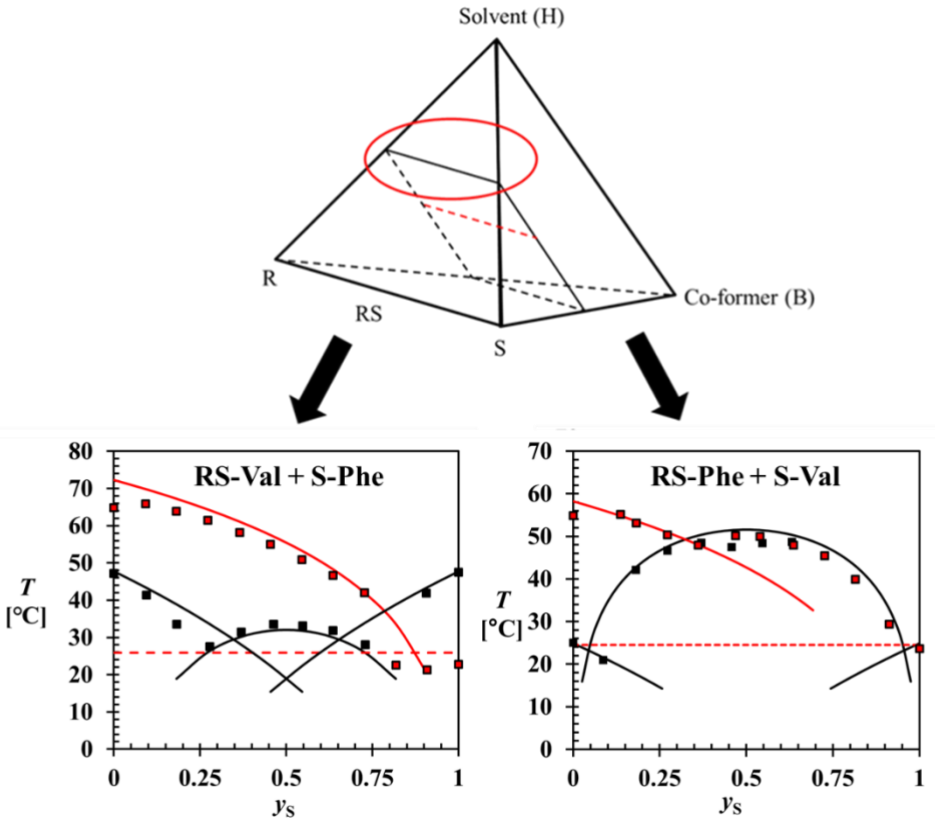

Figure 5. Top: Schematic demonstration of the compositional pyramid of a quaternary system of the target chiral compound consisting of enantiomers R and S, the co-former B and the solvent H. The black line crossing the HRS plane and the red dashed line represent the compositions in type-II pseudo-binary phase diagrams of A in H, in absence and presence of the co-former B, respectively. Bottom left: Type-II pseudo-binary phase diagrams of RS-Val showing saturation temperature T_s versus enantiomer fraction y_S at x_{Val} = 7.6 mmol/mol in absence (left, black) and presence of co-former S-Phe (x_{Phe} = 2.3 mmol/mol) (left, red). Bottom right: Type-II pseudo-binary phase diagrams of RS-Phe (x_{Phe} = 2.3 mmol/mol) in absence

(right, black) and presence of co-former S-Val (x_{Val} = 4.4 mmol/mol) (right, red) in a 20/80 %v/v ethanol/water mixture. The dashed lines indicate the predicted saturation temperature of the co-formers. The black solid lines are predicted saturation temperatures T_s of Val (left) and Phe (right), estimated from Equation.2. The red solid lines are theoretical T_s of co-crystal S-Phe:R-Val (left) and S-Val:R-Phe (right) estimated from Equation. 2 using the Type 1 data.

Type-II Pseudo-binary Phase Diagram. A Type-II pseudo-binary phase diagram illustrates the change in solubility in a three or four component mixture in which only the ratio between the two enantiomers of the target chiral compound is varied. The shape of the phase diagram, especially the number and the location of its eutectic points, provides information about the types of the corresponding co-crystals[6] and the potential for chiral separation.

The top of Figure 5 shows the compositional pyramid of the quaternary system of the 2 enantiomers, co-former B and solvent H. Through the black and red lines it shows the compositions for 2 Type II pseudo-binary phase diagrams. The black line across the HRS plane represents the compositions of a constant total molar fraction of the target chiral compound and a varying R/S ratio in absence of conformer B. The red dashed line in the interior of the pyramid represents the same total molar fraction of the target chiral compound but now in the presence of a specific molar fraction of the co-former B.

RS-Val+S-Phe System. At the bottom left of figure 5 two Type-II pseudo-binary phase diagrams of the target chiral compound Val in 20/80 v/v % ethanol/water in absence (black) and presence (red) of the co-former S-Phe are shown. The measured saturation temperature T_s of each composition is plotted against the target compound S-enantiomer fraction $y_S=x_S/(x_S+x_R)$ in the measured sample. On the outer sides, (y_S < 0.3 and >0.7) the saturation temperatures represent the pure enantiomer crystals R-Val and S-Val, respectively. The symmetrical phase

diagram shows two symmetrical eutectic points located around y_S = 0.3 and 0.7. Between the two eutectic points the racemic compound RS-Val is the more stable crystalline phase.

By adding the co-former S-Phe (x_B=2.3 mmol/mol), an asymmetrical type II pseudo-binary phase diagram is obtained in Figure 5 (left, red). This is because S-Phe only co-crystallizes with R-Val and not with S-Val. For high y_S>0.8, the saturation temperature of roughly 25°C indicates that instead of S-Val, S-Phe crystallized in the samples despite it being slightly less stable than S-Val. However, in a large region ($0 < y_S < 0.8$) of the phase diagram the elevated sample saturation temperatures are higher in the presence of co-former compared to those without the co-former which shows that the co-crystal R-Val:S-Phe is more stable than both the RS-Val and R-Val crystal phase. The presence of the co-crystal in racemic Val solutions was confirmed with XRPD (see EIS). This indicates that in a racemic Val solution containing the right amount of S-Phe, R-Val can selectively be separated by co-crystallization of the co-crystal R-Val:S-Phe.

RS-Phe+S-Val System. Similar to that of Val, the type II pseudo binary phase diagram of Phe in Figure 5 (right, black lines) also contains two symmetrical eutectic points. Noticeably, since the solubility of RS-Phe is significantly lower than that of the pure enantiomer, the racemic Phe is the stable crystalline phase in a larger region in the phase diagram ($0.1 < y_S < 0.9$) compared to racemic Val.

In the presence of the co-former S-Val (4.4 mmol/mol) in the Phe system (Figure 5, right, red lines), the co-crystal R-Phe:S-Val is the most stable compound from y_S = 0 to 0.35. At higher y_S, RS-Phe is the most stable compound. The powder pattern of the solid phase obtained from racemic Phe solutions in the presence of S-Val consists of a mixture of pure RS-Phe and co-crystal R-Phe:S-Val (see Figure SII in ESI). In order to obtain a pure R-Phe:S-Val co-crystal from racemic Phe solutions the concentration of the co-former should be increased so that the co-crystal is stable under racemic conditions. In the Type I phase diagram of R-Phe and S-Val

(Figure 4, left bottom), the theoretical phase diagram of the co-crystal region gives the relationship between the saturation temperature T_s and the molar fraction product $x_{Phe} \cdot x_{Val}$, by using Equation 2 and the values of parameter ΔH and T_0 from Table 2. In order to have a stable R-Phe:S-Val co-crystal whose saturation temperature T_s is higher than that of the pure RS-Phe solution (49°C), the concentration of the co-former S-Val is estimated to be more than 6 mmol/mol, around 40% higher than the level present in the phase diagram in Figure 5 (right bottom).

3.2. Co-crystals using Achiral Co-formers.

Ibuprofen (IBU) is a commonly used nonsteroidal anti-inflammatory drug (NSAID) and S-IBU is over 100-fold more bioactive than the R-enantiomer.[33-34] RS-IBU crystallizes as a stable racemic compound and Figure 6 shows that the solubility of the racemic IBU is significantly lower than its pure enantiomer in Heptane. To investigate co-crystal phase diagram behavior of RS-IBU and achiral co-formers, two achiral co-formers, BPN and BPE, were screened to identify their co-crystal types.

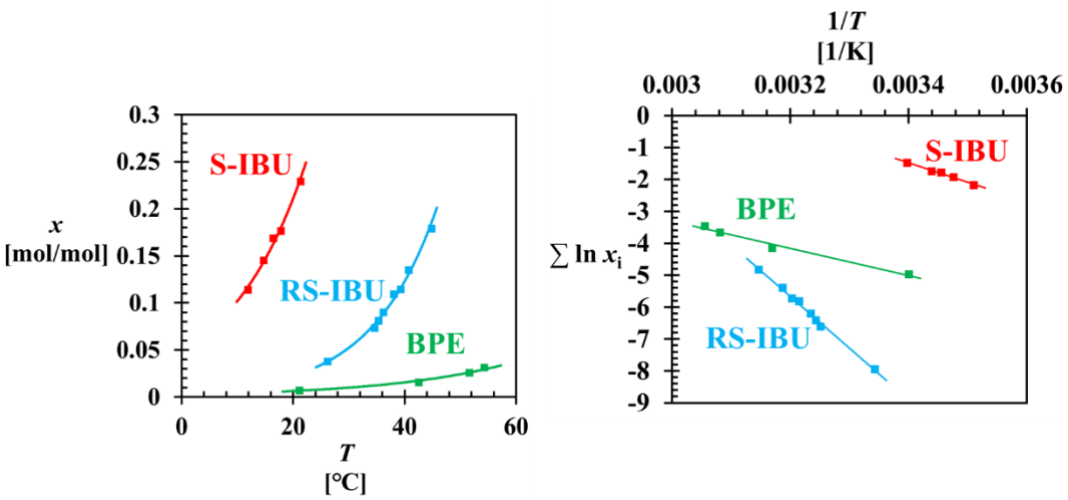

Figure 6. Left: Solubility of RS-IBU, S-IBU and BPE in Heptane (left) as a function of temperature. Right: The summations of natural logarithms of equilibrium molar fractions x_i of each compound i are linear functions of the inverse of temperature T. The solid lines are a linear regression of the experimental data points.

IBU:BPN Co-crystal. Solubility data of the achiral co-former BPN in Heptane could not be reproducibly obtained from saturation temperature measurements because of the severe fluctuation of light transmission signals, probably from the crystals floating on the liquid-air interface in the vials. However, a rough estimate of the co-former BPN in Heptane was obtain to be less than 5 mg/ml at room temperature.

As a reliable solubility data of the co-former is not available, a short-cut approach was employed to quickly determine the type of co-crystals formed from IBU and BPN. In this short-cut approach, two Heptane mixtures were prepared, one containing RS-IBU + BPN and the other S-IBU + BPN. In both mixtures, the concentrations of RS-IBU and S-IBU were 180 mg/ml and the BPN concentration was chosen at 40 mg/ml. The saturation temperature of the RS-IBU + BPN mixture is around 49°C and that of S-IBU + BPN is approximately 40°C. The saturation temperatures of RS-IBU and S-IBU of 180 mg/ml are around 36°C and 12°C, respectively. Therefore, the saturation temperature T_s of the mixtures from RS- and S-IBU are respectively 13 and 28°C higher than those of the pure IBU. Moreover, although the solubility of BPN is unknown, the different T_s of the two mixtures, which contain equal concentrations of the co-former, indicates that these T_s are not of the pure component BPN. Therefore, it is likely that the solid phases from these two mixtures contain co-crystals from IBU and BPN.

This indication of co-crystal formation is confirmed by an XRPD analysis of the solid phases recovered from the two mixtures at room temperatures (see details in ESI). The powder patterns of the solid phases from both mixtures are different from those of the pure component IBU and BPN, indicating that the solid phases are co-crystals. Additionally, the two XRPD patterns of the co-crystals are different from each other, suggesting that the IBU:BPN co-crystal system is a racemic compound system rather than a conglomerate system.

BPN and RS-IBU are reported to co-crystallize as a racemic compound (see crystal structure in Figure 7, top).[35] We further obtained single co-crystals of S-IBU:BPN for single crystal XRD analysis. The obtained 1:2 S-IBU:BPN co-crystal structure is monoclinic with the space group C2 (#5) and unit cell parameters a= 18.2165(12) Å, b= 5.5960(4) Å, c= 33.393(2) Å, β= 92.075(2)°, V= 3401.8(4) Å^3 and with Z=4 asymmetric units in the cell. The asymmetric unit contains one molecule of BPN and two IBU molecules of S-IBU, leading to a 1:2 ratio for the two compounds BPN and S-IBU. The structure of the enantiopure IBU:BPN co-crystal is significantly different from that of the racemic one, which has a space group of $P\bar{1}$(#2) and different dimension of the unit cell (e.g., V = 853.26 Å^3).

An intermolecular hydrogen bond is formed between the hydroxyl groups of the IBU molecules and both Nitrogen atoms at the pyridine groups of BPN (see structure in Figure 7, middle). The generated powder patterns from the racemic and enantiopure co-crystal structure data match those measured in the short-cut approach, indicating that the measured saturation temperatures T_s correspond to the solubilities of the co-crystals (see Figure SIII in ESI).

In a short-cut approach, the screening procedure stops when the single-crystal structure is obtained. However, one of the goals of this study is to demonstrate that the Type-II pseudo-binary phase diagrams of different types of co-crystals are distinctive, thus being feasible as a screening tool. Therefore, the Type-II pseudo-binary phase diagram of the IBU:BPN system is constructed and shown in Figure 8.

The Type-II pseudo-binary phase diagram in absence of the co-former (black) was constructed with a constant total concentration of 180 mg/ml IBU (x_{IBU} = 111 mmol/mol) and a varying S-enantiomer fraction y_S. The phase diagram shows that IBU in Heptane is a racemic compound system and the racemic form is significantly more stable than the pure enantiomer solid: The saturation temperature T_s of the racemic composition is approximately 30°C higher than that of pure R- or S-enantiomer.

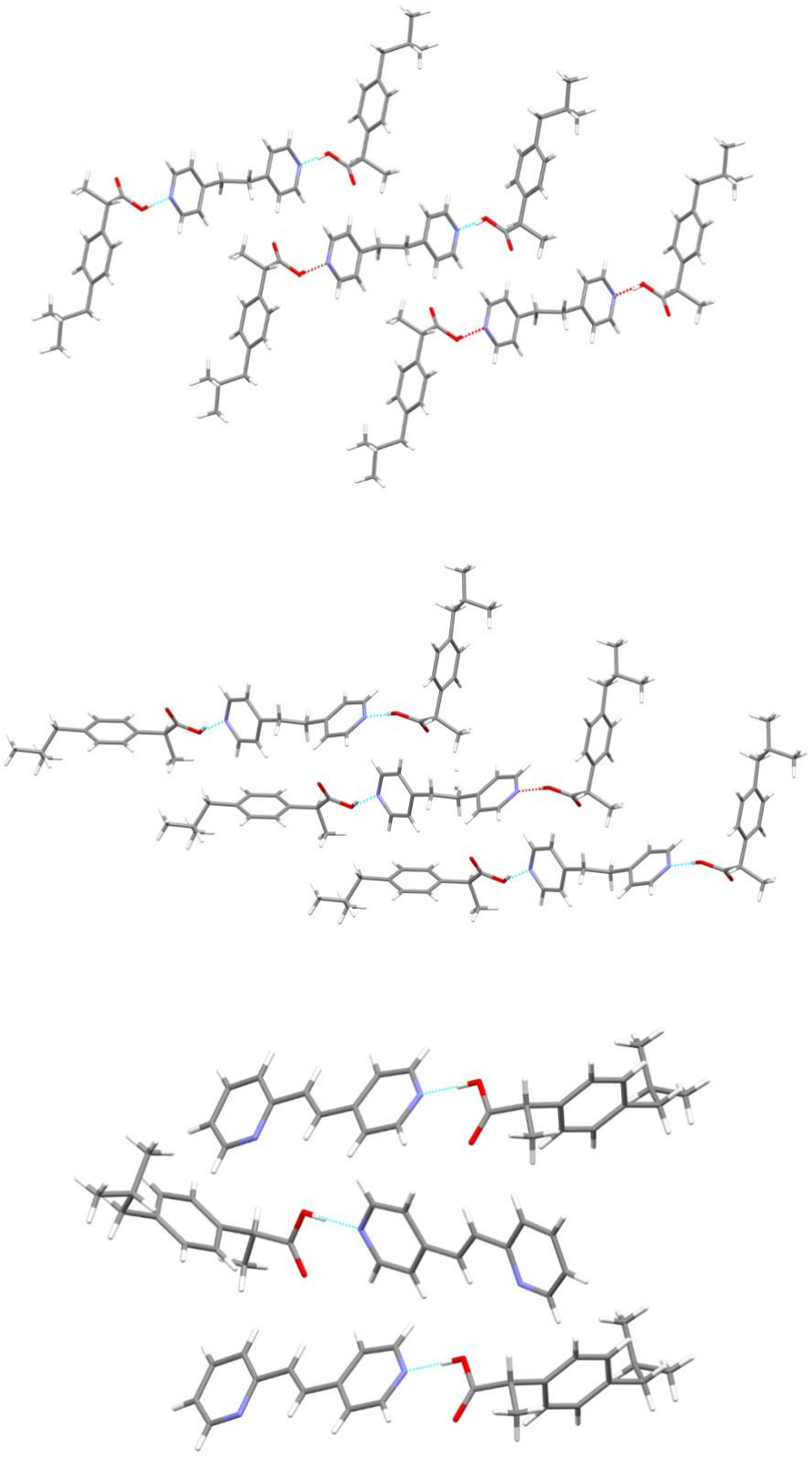

Figure 7. Structure of co-crystals RS-IBU:BPN (top)[35], S-IBU:BPN (middle) and enantiopure IBU:BPE (bottom).

The saturation temperatures in between the two eutectic points, y_S = 0.05 and 0.95, are associated to the racemic compound RS-IBU. Enantiopure S- or R-IBU crystals can only be recovered from a system in which more than 95% of the IBU is composed of the corresponding enantiomer. The solubility lines of racemic IBU and the two enantiomers predicted from the pure compound solubilities in figure 6 are shown as black solid lines in Figure 8 as well. Since the solubility of RS-IBU is significantly lower than that of either enantiomer, the racemic IBU is the dominant solid phase across a large part of the phase diagram. However, the measured phase diagram shows an increase of RS-IBU solubility compared to the predicted one: The presence of the excess of S-enantiomer seems to influence the actual solubility towards higher values.

Figure 8 also shows the type II pseudo-binary phase diagram of 180 mg/ml (114 mmol/mol) IBU in the presence of a constant BPN co-former concentration of 40 mg/ml (x_{BPN} = 28 mmol/mol). The saturation temperature T_s at the racemic composition increased by approximately 15°C while that of the enantiopure form increased by more than 30°C. Although the racemic form is still more stable within a large y_S range, the eutectic points moved closer towards the middle (from y_S = 0.05 and 0.95 to y_S = 0.1 and 0.9).

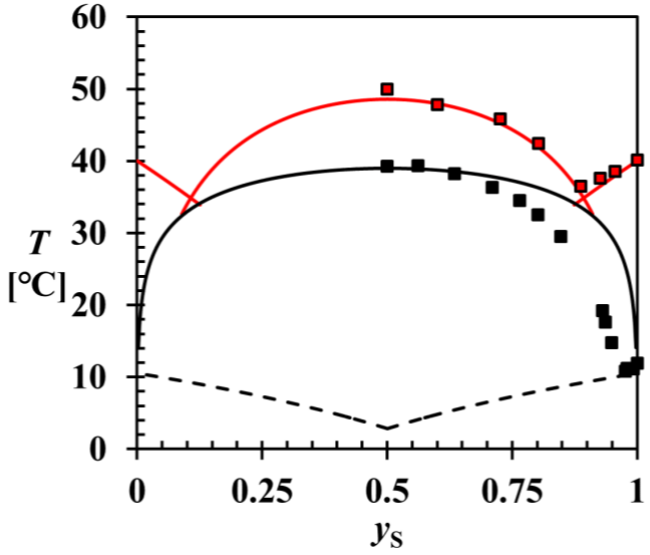

Figure 8. Type-II pseudo-binary T_s, y_S phase diagrams of IBU (black) and IBU-BPN (red) in Heptane. In both phase diagrams the total concentration of IBU was 180 mg/ml (x_{IBU} = 114

mmol/mol). In the IBU-BPN phase diagram (red) the concentration of the co-former BPN was 40 mg/ml (x_{BPN} = 28 mmol/mol). The points are saturation temperature measurements and the lines are predicted from pure racemic compound solubilities (black solid), pure S- or R-IBU (black dashed) as well as of co-crystals (red solid) using Equation. 2.

IBU:BPE Co-crystal. The solubility of the second achiral co-former, trans-1-(2-pyridyl)-2-(4-pyridyl)-ethylene (BPE), is significantly lower than that of IBU. As can be seen from Figure 6 (left), at the same temperature, the solubility of RS-IBU is at least 4 times higher than that of BPE, while the S-IBU solubility is even higher (e.g., at 20°C, solubilities of BPE, RS-IBU and S-IBU are around 8, 35 and 370 mg/ml, respectively). Such a large solubility difference between the target compound A and the co-former B can lead to a Type-I pseudo-binary phase diagram with a eutectic point very close to one side due to the huge excess of IBU.

In order to verify co-crystal formation between IBU and BPE, saturation temperatures T_s of mixed RS-IBU and BPE samples in Heptane were measured. In Figure 9 (left), the temperature differences T_s - T_r of mixtures of RS-IBU and BPE in Heptane were all substantial, which indicates the existence of a stable co-crystal IBU-BPE. In addition, the powder pattern (see ESI) of the solid phases collected for y_s=0.5 indicate a solid phase different from IBU and BPE. It is noticeable in Figure 9 (left) that the temperature difference T_s - T_r decreases as the reference temperature T_r increases. It can be seen from Figure 6 that BPE's solubility is significantly less sensitive to the temperature compared with IBU, which means that the increase of T_r in Figure 9 (left) is accompanied with a change in the sample solution stoichiometry of the two

compounds. Therefore, the decrease of T_s – T_r, along with the increasing IBU/BPE ratio, indicates an influence of the presence of IBU on the solubility of the co-crystals.

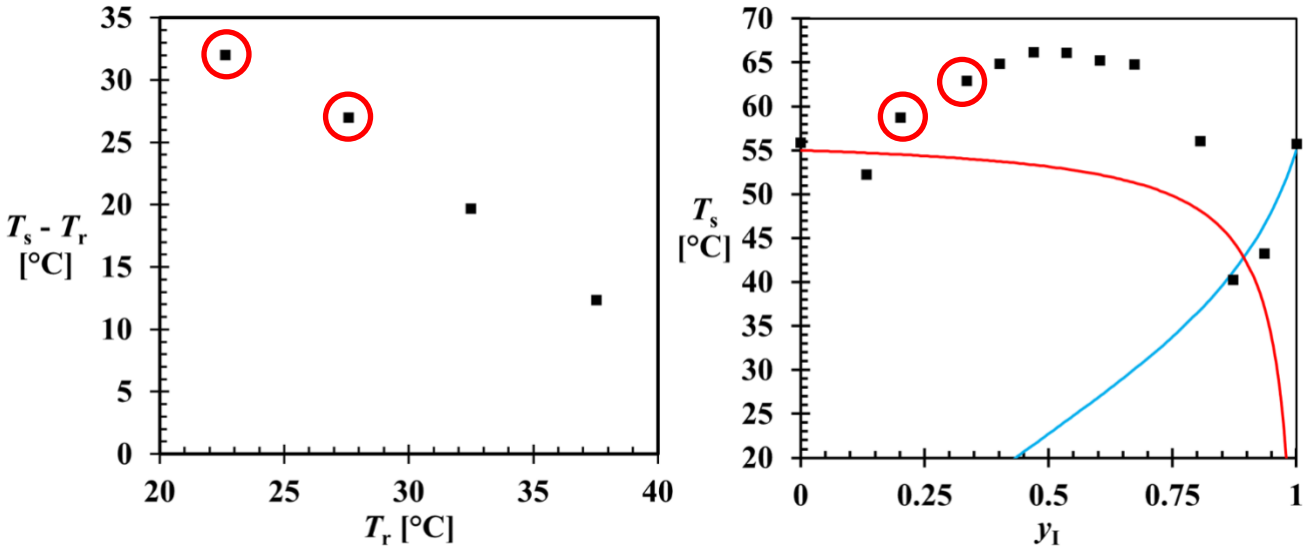

Figure 9. Left: The temperature difference (T_s - T_r) of samples with composition ($x_{RS\text{-}IBU}$*(T_r), x_{BPE}*(T_r)) versus the reference temperature T_r. Right: Type I pseudo-binary phase diagram of measured saturation temperature T_s as a function of solvent-excluded molar fraction of RS-IBU y_I=x_{IBU}/(x_{IBU} +x_{BPE}) from RS-IBU-BPE mixtures in Heptane. The molar composition of $x_{RS\text{-}IBU}$ and x_{BPE} follow Eq. 1. The solid lines are theoretical saturation temperature of pure RS-IBU (blue) and BPE (red) estimated from Eq. 2.

Furthermore, a Type-I pseudo-binary phase diagram is constructed from RS-IBU and BPE in Heptane (Figure 9, right). The measured saturation temperatures T_s of mixtures of RS-IBU and BPE in Heptane are plotted as a function of the solvent-excluded molar fraction y_{IBU} of RS-IBU. The increased saturation temperature T_s between $0.2 < y_{IBU} < 0.8$ indicates the existence of a co-crystal region. Further evidence for co-crystal formation is provided by the XRPD patterns from specific samples in this region (see Figure SIV in ESI), which indicate a solid phase different from those of the pure component crystals. Interestingly, the maximum T_s of the co-crystal is not at the theoretical eutectic point of RS-IBU and BPE (y_I = 0.9 in Figure 9, right), but instead is at around the middle of the phase diagram. This observation is in line

with that from Figure 9 (left), which suggests that the presence of an excess of IBU significantly increases the solubility of the co-crystals.

Following the confirmation of co-crystal formation between RS-IBU and BPE, a Type-II pseudo-binary phase diagram is constructed, in order to identify the co-crystal type. Saturation temperatures of samples with the same concentration of total IBU of 180 mg/ml (x_{IBU} = 114 mmol/mol) and BPE of 40 mg/ml (x_{BPE} = 28 mmol/mol), but varying enantiomer molar fraction $y_S = x_S/(x_S+x_R)$ are determined and plotted (red) in the phase diagram in Figure 10. The phase diagram (black) of only IBU of the same total concentration is also shown in Figure 10 as comparison.

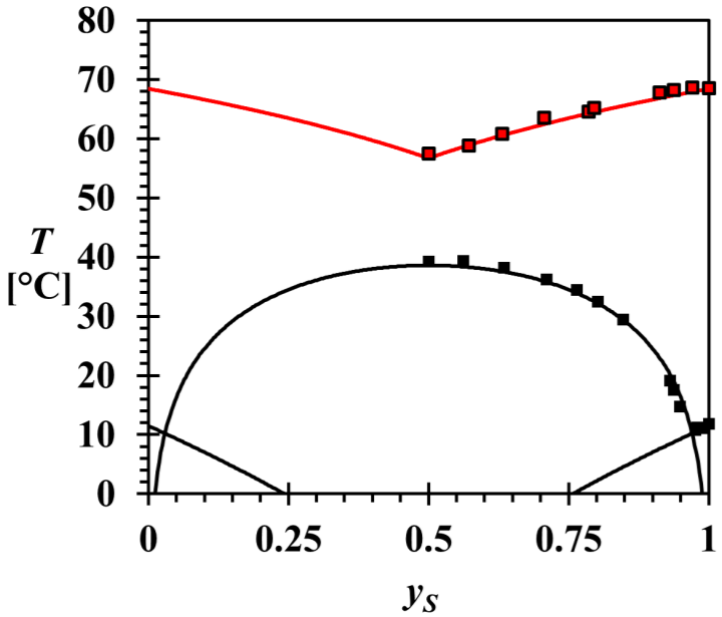

Figure 10. Type II pseudo-binary phase diagrams of IBU (xIBU = 114 mmol/mol, black) and IBU-BPE (xIBU = 114 mmol/mol and xBPE = 28 mmol/mol, red) in Heptane. The graph shows the saturated temperature Ts as a function of y_S, the molar fraction of the S-enantiomer in total IBU. The red solid lines indicate the solubility of the enantiopure co-crystal R- or S-IBU-BPE, estimated from Equation 2. The black solid lines are theoretical phase diagrams of pure component IBU crystals.

The Type-II pseudo-binary phase diagram of IBU and BPE in Heptane in Figure 10 demonstrates a typical feature of a conglomerate system: only one eutectic point can be found

at the racemic composition (y_S=0.5) of the phase diagram. When the system is enriched with either enantiomer at the same total IBU concentration, the saturation temperature T_s is elevated. The estimated phase diagram (red solid line) also indicates the solubility of the enantiopure co-crystal. Two solid samples were taken at room temperature from the samples at y_S=0.5 and 1 in Figure 10 and analyzed using XRPD. This shows that the crystalline phases from these two samples were a mixture of the same co-crystals with either the racemic or the enantiopure IBU (see Figure SV in ESI). These results strongly indicate that IBU and BPE co-crystallize as conglomerates. Additionally, this conglomerate co-crystal system is special as the racemic IBU is significantly more stable than its enantiopure IBU but its enantiopure co-crystal is more stable.

As a last step, single crystals were formed from racemic IBU and BPE in ethanol for co-crystal structure determination. The single co-crystal structure is monoclinic with the chiral space group $P2_1$ (#4), a= 6.4896(2), b= 9.5675(6), c= 17.5232(10) Å, β= 99.892(4)°, V= 1071.83(10)Å^3 and Z=2 (see crystal structure in Figure 7, bottom). This structure is the same as the one reported in literature[17] and generates a simulated powder pattern that can be found back in the experimental patterns from the experiments in figure 10 (see ESI for powder patterns). The single co-crystal structure from the racemic IBU and BPE contain only one of the two IBU enantiomers, the system can thus be identified as conglomerate co-crystal.

The asymmetric unit contains one molecule of BPE and one molecule of enantiopure IBU, leading to a 1:1 ratio for IBU and BPE. An intermolecular hydrogen bond is formed between the hydroxyl group of the carboxylic acid of the IBU molecule and the pyridine nitrogen at the four position of BPE. IBU has a pKa=4.91 while that of BPE can be estimated to be pKa=5.5, assuming a pKa value equal to that of its structural isomer, trans-1,2-bis(4-pyridyl)ethylene[36], indicating that co-crystals rather than salts are formed between the two compounds.

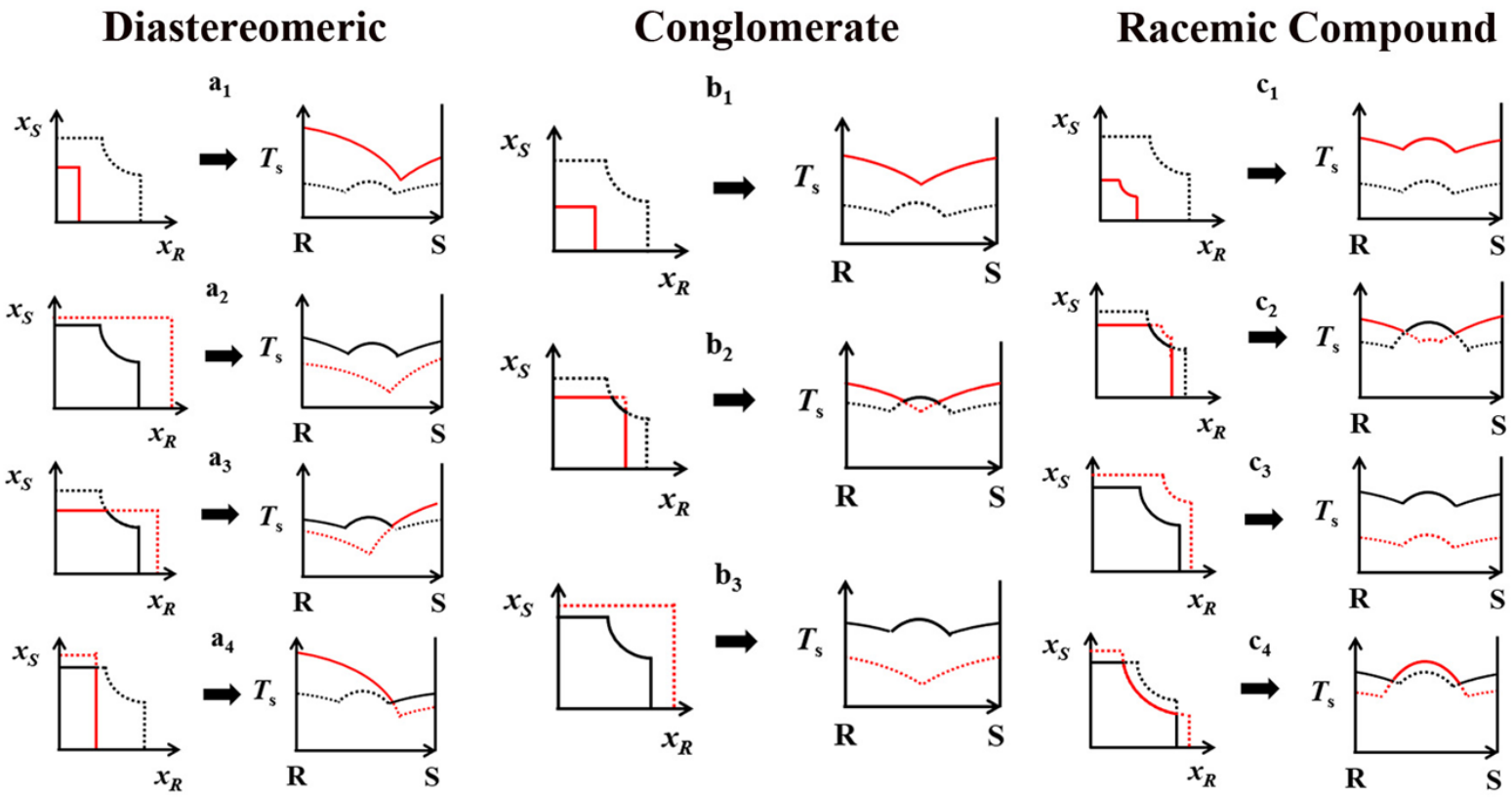

Scheme 2. Schematic isothermal phase diagrams of a racemic compound RS system without (black lines) or with (red lines) a particular amount of co-former (either chiral C or achiral N). On the right of the isothermal phase diagram the corresponding Type II pseudo binary phase diagram is shown. The co-former can be chiral, leading to diastereomerically related co-crystal phases or achiral leading to conglomerate or racemic compound co-crystals. The solid lines indicate solubilities of the most stable compounds while the dashed lines indicate those of the less stable compounds in the presence of the co-former.

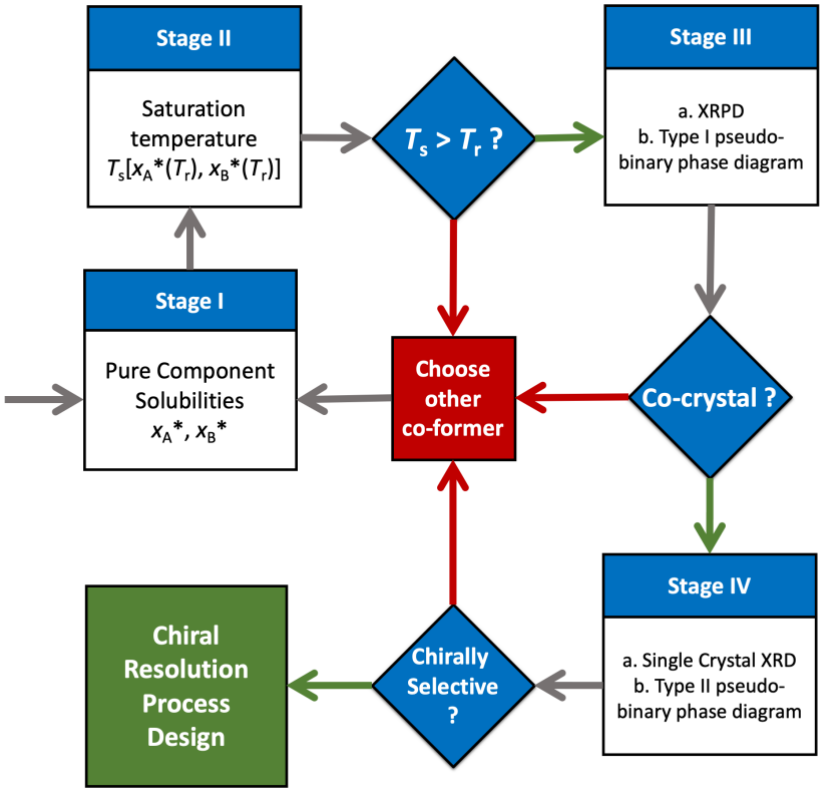

Scheme 3. The screening stages for solids for chiral resolution opportunities based on phase diagram behavior of new enantioselective solids. In stage I the temperature dependent pure component solubilities x_A^* and x_B^* of the target racemic molecule A and the co-former B are determined. In stage II, these solubilities at a series of particular reference temperature T_r are used to measure the saturation temperatures $T_s[x_A^*(T_r),x_B^*(T_r)]$ of the sample series with compositions $[x_A^*(T_r),x_B^*(T_r)]$. If $T_s>T_r$ it is likely a new more stable solid has formed. In stage III XRPD or other solid state analysis tools and phase diagram behavior from a Type I pseudo-binary phase diagram will confirm co-crystal formation. The Single Crystal XRD and Type-II Pseudo-binary phase diagram in Stage IV lead to information on the chiral selectivity potential for the new solid that can be exploited in a chiral resolution process design. Each question in the question box results in a yes (green arrow) or a no (red arrow).

4. DISCUSSIONS

We have identified three different co-crystal types, a diastereomerically related co-crystal, a racemic compound co-crystal and a conglomerate co-crystal, all formed from a racemic solution containing the co-former.

Co-crystal variation. For each type of co-crystal, more composition possibilities exist and the corresponding isothermal and Type-II pseudo-binary phase diagrams are schematically summarized in Scheme 2. In the isothermal phase diagrams, the black lines show the solubility lines in a racemic compound system in absence of co-former B (either chiral or achiral): the horizontal and vertical lines represent the equilibrium solution composition in case of a liquid-solid equilibrium between the solution and pure S and R crystals, respectively. The curved line shows the equilibrium solution composition in case of a liquid-solid equilibrium between the solution and the racemic compound crystals. The intercept between the two straight lines and curved line indicates the eutectic composition at which a three phase equilibrium exists between the solution, the racemic crystal and the enantiopure crystal R or S. All red lines show the solubility lines of the same systems in the presence of a constant amount of B: the red solid lines indicate more stable solids and the red dashed lines indicate less stable solids than those in absence of B.

Similarly, in a Type-II pseudo-binary phase diagram, the black lines, solid or dashed, show the solubility of the target compounds, racemic or enantiopure, without the co-former B. In the presence of a co-former B of a constant molar fraction, a new liquid-solid equilibrium is established in the system, represented by a new phase diagram (red). The solid or dashed red lines indicate the solubility of crystals more or less stable than those without the co-former, respectively.

Phase diagrams a_1—a_4 demonstrate the equilibrium solution composition of diastereomerically related co-crystals R:B and S:B, such as the Phe-Val system. In a_1, both R:B

and S:B co-crystals are more stable than the pure component crystals. Therefore, the red solid lines indicate the solubilities of the R:B and S:B co-crystals, which are different since the co-crystals are diastereomerically related. In a_2, both R:B and S:B co-crystals are less stable than the pure component crystals. The solubilities of the more stable pure component crystals are suggested by the black solid lines. In a_3, the S:B co-crystal is more stable than the S crystal but less stable than the RS crystal. Moreover, the R:B co-crystal is less stable than the pure component crystals. The mixture of RS-Phe+S-Val in Figure 5 (right) is an example of a_3. In a_4, the R:B co-crystal is more stable than both the RS and the R crystals but the co-crystals S:B are less stable than the S crystals. In this case, the phase diagram in the racemic or R-enantiomer enriched region suggests the solubility of the R:B co-crystals while the rest of the phase diagram indicates the solubility of the S crystals. A typical a_4 system is the RS-Val+S-Phe mixture in Figure 5 (left).

When an achiral co-former is used, the co-crystals formed are either conglomerates (Type 2 in Scheme 1) or racemic compounds (Type 3 in Scheme 1), with the rare exceptions of solid solution. Phase diagrams b_1—b_3 show the phase behavior of conglomerate co-crystals S:B and R:B (type 2 in Scheme 1). The phase diagram b_1 describes the situation in which the enantiopure co-crystals are more stable than the pure RS crystals (such as in the case of RS-IBU+BPE system in Figure 10) . Therefore, the phase diagram (red solid lines) suggest the solubilities of the two enantiopure co-crystals. In b_2, the RS crystals are still more stable than the enantiopure co-crystals in the region close to the racemic composition. Although the phase diagram with the co-former B (solid lines) is similar to the pure component phase diagram, the parts on the two sides of the eutectic points (solid red lines) show the solubilities of the enantiopure co-crystals. In b_3, the co-crystals are less stable than the pure component crystals. Therefore, the phase diagram with the presence of the co-former B is the same as that without.

Phase diagrams c_1—c_4 describe the phase behaviors of racemic compound co-crystals RS:B (type 3 in Scheme 1). In c_1, both the racemic co-crystals RS:B and the enantiopure co-crystals R:B and S:B are more stable than the pure component crystals, for instance as in the case of RS-IBU+BPN system in Figure 8. The phase diagram (solid red lines) suggests the solubilities of the co-crystals. In c_2, the enantiopure co-crystals are more stable than the S or R crystals but the RS crystals are still more stable than the co-crystals in the region close to the racemic composition. Therefore, the parts of the phase diagram on the two sides of the eutectic points (solid red lines) show the solubilities of co-crystals R: or S:B while the region close to the middle indicates the RS crystals solubility. In c_3, the co-crystals are less stable than the pure component crystals and the phase diagram with the co-former B is the same as that without. In c_4, the RS:B co-crystals are more stable than the corresponding pure component crystals RS but the enantiopure R:B or S:B co-crystals are less stable than either R or S crystals. Therefore, the section between the eutectic points represents the solubility of the RS:B co-crystals while the two sides indicate that of the enantiopure pure component crystals R and S.

In addition to identifying co-crystal types, a Type-II pseudo-binary phase diagram also provides guidelines for the conceptual design of suitable chiral separation processes. Figure 5 gives suggestions on the chiral resolution of either Phe or Val. In absence of the chiral co-former, the recovery of enantiopure Val or Phe cannot be achieved from their racemic solutions due to racemic compound formation. By adding 18 mg/ml of the chiral co-former S-Phe, in a solution of Val (c_{Val} = 42 mg/ml), R-Val can be recovered in the form of R-Val:S-Phe co-crystals, even when the original solution is racemic. The cooling crystallization of R-Val:S-Phe can be operated until around 30°C, which is the T_s of pure RS-Val. Below this temperature, the nucleation of RS-Val can contaminate the co-crystal product. In the case of Phe, without the co-former S-Val, R-Phe can be recovered by cooling crystallization if the solution is enriched so that $y_S < 0.1$. By adding 24 mg/ml co-former S-Val, R-Phe can be recovered as R-

Phe:S-Val co-crystals as long as the original solution has an enantiomeric excess $E > 0.4$ (corresponding to $y_S < 0.3$). It is estimated from Equation 2 that if the amount of S-Val increases to around 35 mg/ml S-Val, R-Phe:S-Val co-crystals can be recovered from a racemic Phe mixture.

The achiral co-former BPN co-crystallizes with IBU as racemic compounds, which is not ideal for chiral separation techniques. However, the change in the position of the eutectic points can still reduce the requirement for the application of chiral separation: for instance, without co-crystallization, preferential crystallization could be applied on the IBU system if the solution is enriched with 95% of S-enantiomer, for instance by chiral chromatography[37]. With the co-former BPN, the requirement of enrichment is decreased to only 90%. Therefore, with a racemic compound co-crystal, a relatively less demanding chiral separation process can be designed.

Co-crystals for Resolution. With the structural information from the single crystal, IBU is confirmed to co-crystallize as a conglomerate using the co-former BPE. The IBU:BPE co-crystal is, to our knowledge, the second conglomerate co-crystal structure reported from a racemic compound, after the system of Naproxen-Nicotinamide[16]. The conversion from the racemic compound IBU to the conglomerate-forming IBU:BPE co-crystal enables the application of chiral separation techniques such as preferential crystallization. For instance, if a Heptane solution of IBU, with total concentration of 180 mg/ml, contained an initial enantiomeric excess E (e.g., $E = 6\%$), a direct crystallization step cannot recover enantiopure solid phase as can be seen from the phase diagram (black) in Figure 10. However, by adding 40 mg/ml BPE into the system, the initial enantiomeric excess can all be recovered as enantiopure IBU:BPE co-crystals.

Although other co-crystals identified in this study are not conglomerate, they can still potentially be resolved. In the racemic solution in figure 5 (left) there is sufficient chiral co-

former present to make the enantiopure co-crystal compound more stable than the racemic compound. Under these conditions one enantiomer is selectively crystallized while the other remains in solution. In figure 8 the racemic co-crystal is more stable than the racemic compound resulting in a eutectic point shift which might enable integrated techniques such as chromatography and crystallization to be exploited.

Co-crystallization provides opportunities for chiral separation of racemic-compound-forming molecules. Type-II pseudo-binary phase diagrams can be used to identify the types of co-crystals from racemic compounds, as has been proven by the three systems investigated in this study. Based on this result, a systematic screening method has been developed to search for suitable co-crystal combinations of the target compounds for chiral separation opportunities. A schematic demonstration of the newly developed screening method is shown in Scheme 3.

Stage I—III in the screening method is to identify the formation of co-crystals between the target chiral compound (A) and the selected co-former (B), as described by ter Horst *et al.* in a previous study on discovering new co-crystals.[26] The enantiomer of A is used if B is chiral and a racemic mixture of A is used if B is achiral.

In stage IV, the type of co-crystals are determined either by a Type-II pseudo-binary phase diagram or by Single-Crystal XRD (SCXRD) or both. If applicable, the Type-II pseudo-binary phase diagrams (see the complete list of possible phase diagrams in Scheme 2) are used to select a suitable chiral separation technique for the target chiral compound.

In the case of B being an achiral co-former, a short-cut approach can be employed for quick screening, such as in the case of IBU + BPN system in this study. Crystals can be formed from two solutions of compositions [x_A*(T_r),x_B*(T_r)], where A is one enantiomer in one solution and is the racemic mixture in the other. The crystals from the two solutions are then analyzed by XRPD and the obtained powder patterns are first compared with those of pure component

crystals to determine whether co-crystals are formed. If so, the two XRPD patterns are compared with each other to determine whether conglomerate co-crystals are formed, as the patterns are the same from a conglomerate co-crystal system. In the case where solubility data is not available, two mixtures containing equal concentrations of one enantiomer and the racemic mixture of the target compound can be used. This short-cut procedure (see Scheme 3) determines whether or not the combination A-B forms desired co-crystal types without the two pseudo-binary phase diagrams. As a trade-off, relevant guidelines for chiral separation process design provided by Type-II pseudo-binary phase diagrams are not available from the short-cut step.

In pharmaceutical industry, in many cases, undesired co-former might lead to toxicity of the drugs, which hinders the approval and the subsequent launch of these products. This imposes a potential challenge to the chiral resolution techniques mediated by co-crystallization. However, the co-former does not necessarily end-up in the final formulation. In fact, such risks can be mitigated, if needed, via a suitable downstream process, e.g., recrystallization to separate the API with the co-former[12].

5. CONCLUSIONS

A systematic phase-diagram-based screening method to identify the co-crystal types from racemic-compound-forming molecules has been developed and experimentally verified by studying 3 chiral systems. The system of Phe and Val in 20/80 % v/v ethanol/water mixtures form diastereomerically related co-crystals. The non-chiral co-former BPN forms racemic compound co-crystals with IBU. The racemic compound IBU is converted into a conglomerate co-crystal by using the non-chiral co-former BPE. These three chiral compound systems have different Type-II pseudo-binary phase diagrams, which can be used to identify their co-crystal types and co-crystallization conditions. Such pseudo-binary phase diagrams enable a structured

exploration of co-crystal phase diagrams of chiral compounds and their chiral separation opportunities.

AUTHOR INFORMATION

Corresponding Author:

Joop H. ter Horst

Email: Joop.terHorst@strath.ac.uk

SUPPORTING INFORMATION

The XRPD diffractograms of all relevant crystalline products from the present study are available in the supporting information.

Author Contributions

The manuscript was written through contributions of all authors. All authors have given approval to the final version of the manuscript.

DATA AVAILABILITY

CCDC 1987385 and 1987386 contain the supplementary crystallographic data for this paper. These data are provided free of charge by The Cambridge Crystallographic Data Centre.

ACKNOWLEDGMENT

J.H.T.H would like to thank the EPSRC and the Doctoral Training Centre in Continuous Manufacturing and Crystallisation (Grant Ref: EP/K503289/1) for funding. This work is part of the CW Programme Grant on “Chiral purification of racemic compounds: a grinding

approach" and was made possible by financial support from The Netherlands Organization for Scientific Research (Nederlandse Organisatie voor Wetenschappelijk Onderzoek (NWO)).

REFERENCES

1. Lorenz, H.; Seidel-Morgenstern, A., Processes To Separate Enantiomers. *Angew. Chem., Int. Ed.* **2014,** *53*, 1218-1250.

2. Rouhi, A. M., Chirality at work. *Chem. Eng. News* **2003,** *81*, 56-61.

3. Ward, T. J.; Ward, K. D., Chiral Separations: A Review of Current Topics and Trends. *Anal. Chem.* **2012,** *84*, 626-635.

4. Coquerel, G., Preferential Crystallization. In *Novel Optical Resolution Technologies*, Sakai, K.; Hirayama, N.; Tamura, R., Eds. Springer Berlin Heidelberg: Berlin, Heidelberg, 2007; pp 1-51.

5. Sogutoglu, L.-C.; Steendam, R. R. E.; Meekes, H.; Vlieg, E.; Rutjes, F. P. J. T., Viedma ripening: a reliable crystallisation method to reach single chirality. *Chem. Soc. Rev.* **2015,** *44*, 6723-6732.

6. Srisanga, S.; ter Horst, J. H., Racemic Compound, Conglomerate, or Solid Solution: Phase Diagram Screening of Chiral Compounds. *Cryst. Growth Des.* **2010,** *10*, 1808-1812.

7. Noorduin, W. L.; Kaptein, B.; Meekes, H.; van Enckevort, W. J. P.; Kellogg, R. M.; Vlieg, E., Fast Attrition-Enhanced Deracemization of Naproxen by a Gradual In Situ Feed. *Angew. Chem., Int. Ed.* **2009,** *48*, 4581-4583.

8. Li, W. W.; Spix, L.; de Reus, S. C. A.; Meekes, H.; Kramer, H. J. M.; Vlieg, E.; ter Horst, J. H., Deracemization of a Racemic Compound via Its Conglomerate-Forming Salt Using Temperature Cycling. *Cryst. Growth Des.* **2016,** *16*, 5563-5570.

9. Spix, L.; Alfring, A.; Meekes, H.; van Enckevort, W. J. P.; Vlieg, E., Formation of a Salt Enables Complete Deracemization of a Racemic Compound through Viedma Ripening. *Cryst. Growth Des.* **2014,** *14*, 1744-1748.

10. Wermester, N.; Aubin, E.; Pauchet, M.; Coste, S.; Coquerel, G., Preferential crystallization in an unusual case of conglomerate with partial solid solutions. *Tetrahedron: Asymmetry* **2007,** *18*, 821-831.

11. Horst, J. H. t.; Cains, P. W., Co-Crystal Polymorphs from a Solvent-Mediated Transformation. *Cryst. Growth Des.* **2008,** *8*, 2537-2542.

12. Urbanus, J.; Roelands, C. P. M.; Verdoes, D.; Jansens, P. J.; ter Horst, J. H., Co-Crystallization as a Separation Technology: Controlling Product Concentrations by Co-Crystals. *Cryst. Growth Des.* **2010,** *10*, 1171-1179.

13. Springuel, G.; Leyssens, T., Innovative Chiral Resolution Using Enantiospecific Co-Crystallization in Solution. *Cryst. Growth Des.* **2012,** *12*, 3374-3378.

14. Harmsen, B.; Leyssens, T., Enabling Enantiopurity: Combining Racemization and Dual-Drug Co-crystal Resolution. *Cryst. Growth Des.* **2018,** *18*, 3654-3660.

15. Guillot, M.; de Meester, J.; Huynen, S.; Collard, L.; Robeyns, K.; Riant, O.; Leyssens, T., Cocrystallization-Induced Spontaneous Deracemization: A General Thermodynamic Approach to Deracemization. *Angew. Chem., Int. Ed. Engl.* **2020,** *59*, 11303-11306.

16. Neurohr, C.; Marchivie, M.; Lecomte, S.; Cartigny, Y.; Couvrat, N.; Sanselme, M.; Subra-Paternault, P., Naproxen–Nicotinamide Cocrystals: Racemic and Conglomerate Structures Generated by CO2 Antisolvent Crystallization. *Cryst. Growth Des.* **2015,** *15*, 4616-4626.

17. Elacqua, E. Supramolecular chemistry of molecular concepts:tautomers, chirality, protecting groups,trisubstituted olefins, cyclophanes, and their impacton the organic solid state. PhD thesis, University of Iowa, Iwoa City, IA, 2012.

18. Harfouche, L. C.; Couvrat, N.; Sanselme, M.; Brandel, C.; Cartigny, Y.; Petit, S.; Coquerel, G., Discovery of New Proxyphylline-Based Chiral Cocrystals: Solid State Landscape and Dehydration Mechanism. *Cryst. Growth Des.* **2020,** *20*, 3842-3850.

19. Harfouche, L. C.; Brandel, C.; Cartigny, Y.; Petit, S.; Coquerel, G., Resolution by Preferential Crystallization of Proxyphylline by Using Its Salicylic Acid Monohydrate Co-Crystal. *Chem. Eng. Technol.* **2020,** *43*, 1093-1098.

20. Grothe, E.; Meekes, H.; Vlieg, E.; ter Horst, J. H.; de Gelder, R., Solvates, Salts, and Cocrystals: A Proposal for a Feasible Classification System. *Cryst. Growth Des.* **2016,** *16*, 3237-3243.

21. Springuel, G.; Robeyns, K.; Norberg, B.; Wouters, J.; Leyssens, T., Cocrystal Formation between Chiral Compounds: How Cocrystals Differ from Salts. *Cryst. Growth Des.* **2014,** *14*, 3996-4004.

22. Sánchez-Guadarrama, O.; Mendoza-Navarro, F.; Cedillo-Cruz, A.; Jung-Cook, H.; Arenas-García, J. I.; Delgado-Díaz, A.; Herrera-Ruiz, D.; Morales-Rojas, H.; Höpfl, H., Chiral Resolution of RS-Praziquantel via Diastereomeric Co-Crystal Pair Formation with l-Malic Acid. *Cryst. Growth Des.* **2016,** *16*, 307-314.

23. Berry, D. J.; Seaton, C. C.; Clegg, W.; Harrington, R. W.; Coles, S. J.; Horton, P. N.; Hursthouse, M. B.; Storey, R.; Jones, W.; Friščić, T.; Blagden, N., Applying Hot-Stage Microscopy to Co-Crystal Screening: A Study of Nicotinamide with Seven Active Pharmaceutical Ingredients. *Cryst. Growth Des.* **2008,** *8*, 1697-1712.

24. Chen, S.; Xi, H.; Henry, R. F.; Marsden, I.; Zhang, G. G. Z., Chiral co-crystal solid solution: structures, melting point phase diagram, and chiral enrichment of (ibuprofen)2(4,4-dipyridyl). *CrystEngComm* **2010,** *12*, 1485-1493.

25. Reus, M. A.; van der Heijden, A. E. D. M.; ter Horst, J. H., Solubility Determination from Clear Points upon Solvent Addition. *Org. Process Res. Dev.* **2015,** *19*, 1004-1011.

26. ter Horst, J. H.; Deij, M. A.; Cains, P. W., Discovering New Co-Crystals. *Cryst. Growth Des.* **2009,** *9*, 1531-1537.

27. de Gelder, R.; de Graaff, R. A. G.; Schenk, H., Automatic determination of crystal structures using Karle-Hauptman matrices. *Acta Crystallogr., Sect. A* **1993,** *49*, 287-293.

28. Sheldrick, G., SHELXT - Integrated space-group and crystal-structure determination. *Acta Crystallogr., Sect. A* **2015,** *71*, 3-8.

29. Sheldrick, G., Crystal structure refinement with SHELXL. *Acta Crystallogr., Sect. C* **2015,** *71*, 3-8.

30. Prasad, G. S.; Vijayan, M., X-ray studies on crystalline complexes involving amino acids and peptides. XXI. Structure of a (1:1) complex between l-phenylalanine and d-valine. *Acta Crystallogr., Sect. C* **1991,** *47*, 2603-2606.

31. Moitra, S.; Kar, T., Growth and characterization of L-valine - a nonlinear optical crystal. *Cryst. Res. Technol.* **2010,** *45*, 70-74.

32. Shiraiwa, T.; Ikawa, A.; Sakaguchi, K.; Kurokawa, H., OPTICAL RESOLUTION OF DL-AMINO ACIDS WITH ALIPHATIC SIDE CHAIN BY USING L-PHENYLALANINE. *Chem. Lett.* **1984,** *13*, 113-114.

33. Nguyen, L. A.; He, H.; Pham-Huy, C., Chiral Drugs: An Overview. *Int. J. Biomed. Sci.* **2006,** *2*, 85-100.

34. Chen, C. Y.; Chen, C. S., Stereoselective disposition of ibuprofen in patients with compromised renal haemodynamics. *Br. J. Clin. Pharmacol.* **1995,** *40*, 67-72.

35. Alshahateet, S. F., Synthesis and Supramolecularity of Hydrogen-Bonded Cocrystals of Pharmaceutical Model Rac-Ibuprofen with Pyridine Derivatives. *Mol. Cryst. Liq. Cryst.* **2010,** *533*, 152-161.

36. R Shattock, T. Crystal engineering of co-crystals and their relevance to pharmaceutical forms. PhD thesis. University of South Florida, Tampa, FL, 2007.

37. Welch, C. J. Chiral Chromatography in Support of Pharmaceutical Process Research. In *Preparative Enantioselective Chromatography*; Cox G.B.; Blackwell Publishing Ltd: Hoboken, NJ, 2005; pp 1-18.

For Table of Content Use Only.

A Screening Approach for Identifying Co-crystal Types and Resolution Opportunities in Complex Chiral Multicomponent Systems

Weiwei Li, Mariette de Groen, Herman J.M. Kramer, René de Gelder, Paul Tinnemans, Hugo Meekes and Joop H. ter Horst*

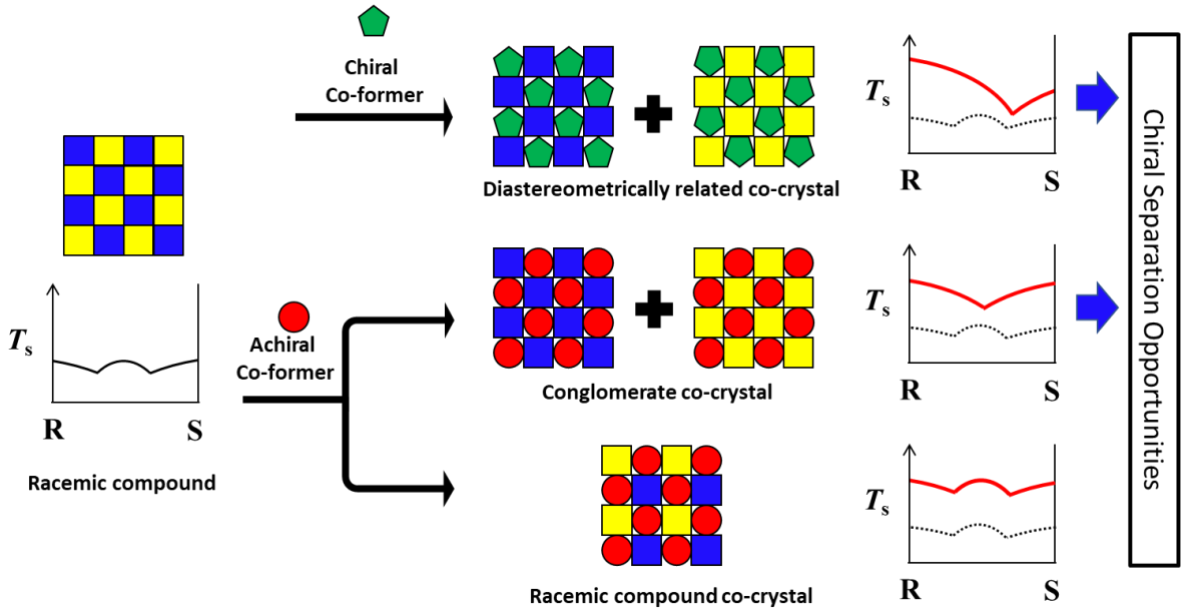

Synopsis:

The present study describes a systematic method to identify the types and phase diagrams of co-crystals formed by chiral target compounds and candidate co-formers in a particular solvent system. Typical phase diagrams of various types of co-crystals are presented. Moreover, the phase diagram diversity and their potential for chiral separation are discussed.